*The Canadian Mineralogist*
Vol. 36, pp. 1237-1244 (1998)

# CONTRASTING PATTERNS OF [6]Al ORDER IN SYNTHETIC PARGASITE AND Co-SUBSTITUTED PARGASITE

GIANCARLO DELLA VENTURA[1]

*Dipartimento di Scienze Geologiche, Università di Roma Tre, Largo S. Leonardo Murialdo 1, I- 00146 Roma, Italy*

JEAN-LOUIS ROBERT

*Centre de Recherche sur la Synthèse et Chimie des Minéraux, C.N.R.S. and FR 09, 1A, rue de la Férollerie, F-45071 Orléans Cedex 2, France*

FRANK C. HAWTHORNE

*Department of Geological Sciences, University of Manitoba, Winnipeg, Manitoba R3T 2N2*

MATI RAUDSEPP

*Department of Geological Sciences, University of British Columbia, 6339 Stores Road, Vancouver V6T 1Z4*

MARK D. WELCH

*Department of Mineralogy, The Natural History Museum, Cromwell Road, London SW7 5BD, U.K.*

## Abstract

Infrared spectroscopy in the principal OH-stretching region and Rietveld refinement indicate that [6]Al is randomly distributed over the *M*(2) and *M*(3) sites in pargasite, whereas [6]Al is strongly ordered at *M*(2) in Co-substituted pargasite. The introduction of Co results in an overall expansion of the structure. However, comparison with unit-cell data of previously reported synthetic pargasite and ferropargasite reveals a marked decrease of the *b* dimension in Co-substituted pargasite; this is a direct result of the different patterns of order of [6]Al in the amphiboles being compared. The degrees of [6]Al disorder observed in synthetic pargasite and Co-substituted pargasite are compatible with the range of disorder observed in analogous natural amphiboles, and are strongly related to the mean radius of the octahedrally coordinated divalent cations.

*Keywords*: pargasite, synthesis, Rietveld refinement, infrared spectroscopy, cobalt, order–disorder.

## Sommaire

Les données sur la fréquence de l'étirement OH en spectroscopie infra-rouge et les résultats d'affinements Rietveld indiquent que l'aluminum en coordinence octaédrique est distribué de façon aléatoire sur les sites *M*(2) et *M*(3) dans la pargasite synthétique, tandis qu'il est fortement ordonné sur *M*(2) dans l'équivalent cobaltifère. L'introduction du Co mène à une expansion généralisée de la structure. Toutefois, une comparaison des paramètres réticulaires déjà dans la littérature pour la pargasite et la ferropargasite synthétiques révèle une augmentation marquée de la dimension *b*, conséquence directe des schémas différents de mise en ordre de [6]Al dans les amphiboles comparées. Le degré de désordre impliquant [6]Al dans la pargasite synthétique et son équivalent cobaltifère concorde avec l'intervalle de degrés d'ordre observé dans les amphiboles naturelles analogues, et reflète étroitement le rayon ionique moyen des cations bivalents en coordinence octaédrique.

(Traduit par la Rédaction)

*Mots-clés*: pargasite, synthèse, affinement Rietveld, spectroscopie infra-rouge, cobalt, ordre–désordre.

[1] *E-mail address*: dellaven@uniroma3.it

## INTRODUCTION

Many investigators have synthesized nominal end-member pargasite (Boyd 1959, Gilbert 1969, Holloway 1973, Semet 1973, Hinrichsen & Schürmann 1977, Braue & Seck 1977, Oba 1980, Westrich & Holloway 1981), and Charles (1980) has synthesized pargasite along the Mg–$Fe^{2+}$ join. More recently, Raudsepp *et al.* (1987) reported the synthesis and characterization by Rietveld and spectroscopic analyses of pargasite analogues with different trivalent octahedrally coordinated constituents. They showed evidence of significantly disordered distributions of trivalent cations (Al,Cr,Sc,In) over the available octahedral sites. Analogous results were obtained by Welch *et al.* (1994) by $^1H$ MAS NMR spectroscopy on end-member synthetic pargasite.

Here, we report the synthesis and characterization of pargasite with two different divalent octahedrally coordinated cations (Mg and Co). The purpose of this work is twofold: (i) to characterize the crystal-chemical behavior of $Co^{2+}$ with regard to Mg, and (ii) to characterize the effect of $Co^{2+}$ *versus* Mg on the distribution of Al over the strip of octahedra.

## EXPERIMENTAL METHODS

### *Synthesis*

Starting materials were prepared as silicate gels according to the method of Hamilton & Henderson (1968). Two compositions were prepared: nominal pargasite, $NaCa_2(Mg_4Al)(Si_6Al_2)O_{22}(OH)_2$, and nominal Co-substituted pargasite, $NaCa_2(Co_4Al)(Si_6Al_2)O_{22}(OH)_2$. Syntheses were done at 700°C, 2 kbar in externally heated cold-seal pressure vessels.

### *Measurement of the X-ray data*

Products of synthesis were ground in an alumina mortar for 30 minutes and mounted in aluminum holders with cavities 20 × 15 × 1.5 mm. In order to minimize preferred orientation, the powder was back-loaded against a frosted-glass slide. The already textured surface was then serrated with a razor blade; this manipulation tends to randomize the orientation of anisotropic crystals that are aligned during filling, but preserves a reasonably flat surface. Step-scan powder-diffraction data were collected using a Philips PW1710 diffractometer with a 1050 Bragg–Brentano goniometer, 0.5 mm divergence and antiscatter slits, a 0.2 mm receiving slit and a curved graphite diffracted-beam monochromator. Information pertinent to data measurement is given in Table 1.

### *Rietveld structure refinement*

The structure of Co-substituted pargasite was refined by the Rietveld method using the program LHPM1 [DBW 3.2, originally written by Wiles & Young (1981) and modified by Hill & Howard (1986)]. For the additional phases (see below), only Co-substituted diopside was introduced into the final cycles, and only the cell parameters and the scale factors were refined; all other structural parameters were fixed. Introducing anorthite resulted in a very difficult refinement and did not affect significantly the final results, particularly the site occupancies. The peaks were refined with pseudo-Voigt profiles with variable percentages of Lorentzian character. The peak full-width at half-maximum height (FWHM) was refined as a function of 2θ using the expression of Caglioti *et al.* (1958). Peaks were corrected for asymmetry using the semi-empirical relation of Rietveld (1969). The intensity at each step of the profile was calculated over an interval of four FWHM on either side of each peak centroid. Backgrounds were fitted with a simple polynomial function. Isotropic-displacement factors were fixed at values approximately correct for amphiboles, and neutral scattering factors were used for all atoms. The *A*-site cation was fixed at the special position 2*b* (*A2/m*). Final convergence was assumed when the parameter shifts in the final cycle were less than 30% of the respective standard deviations.

TABLE 1. DETAILS CONCERNING DATA COLLECTION AND STRUCTURE REFINEMENT OF SYNTHETIC Co-SUBSTITUTED PARGASITE

| | | | |
|---|---|---|---|
| Scan range (°) | 9-100 | N–P | 860 |
| Step interval (°2θ) | 0.10 | $R_p$% | 6.47 |
| Integration time/step | 5 | $R_{wp}$% | 8.48 |
| Structural parameters | 38 | Durbin-Watson *d* statistic | 1.97 |
| Experimental parameters | 13 | space group | *C2/m* |

N–P: number of observations (steps) minus the number of least-squares parameters.

### *Infrared spectroscopy*

FTIR spectra in the principal OH-stretching region (4000–3000 $cm^{-1}$) were collected on a Nicolet 800 spectrophotometer equipped with a nitrogen-cooled MCT detector and a $CaF_2$ beam-splitter; the nominal resolution was 2 $cm^{-1}$. Spectra are the average of 64 scans. Samples were prepared as KBr pellets with a KBr:mineral ratio of 140:10. Details of the sample preparation may be found in Robert *et al.* (1989).

### *Transmission electron microscopy*

HRTEM observations were made using a JEOL 200CX transmission electron microscope operated at 200 kV and having a ±30° tilt about two orthogonal axes. Crystallites were dispersed in dry alcohol and sedimented onto a 3 mm holey-carbon copper grid (Agar products) using a pipette. All samples were found to be very beam-sensitive; a 70 μm condenser-aperture was used to minimize beam damage. High-resolution images

were formed from diffracted beams that passed through a 40 μm (0.45 $Å^{-1}$) objective aperture.

*Electron-microprobe analyses (EMPA)*

Electron-microprobe analysis of Co-substituted pargasite was done using a Cameca SX–50 instrument operated at 20 kV and 15 nA with a beam size of 1 μm. The following standards were used: wollastonite (Ca, Si), metal Co, corundum (Al) and New Idria jadeite (Na).

## Results

*Run products*

For pargasite, a yield of >95% clinoamphibole was obtained, together with minor phyllosilicate. The Co-substituted pargasite run-product consisted of approximately 90% clinoamphibole plus Co-substituted diopside and anorthite. The amphibole crystals are prismatic along *c*, up to 15 μm long and 3–5 μm in diameter, with the majority of the crystals being much smaller. About twenty crystallites of amphibole were imaged by HRTEM. These ranged in size from whole tiny crystallites up to thin edges of larger grains. In general, larger grains are relatively free of polysomatic defects (chain-multiplicity faults, CMFs) and consist of an uninterrupted sequence of double chains with the characteristic 9 Å fringe spacing (Fig. 1a). However, some smaller grains contain many CMFs, with multiplicities of 3 and 4 (Fig. 1b). Attempts were made to reduce the structural defects by increasing the T of synthesis up to 850°C, but HRTEM examination of the resulting run products showed that grains of higher-temperature amphibole had essentially as many defects as those crystallized at the lower temperature.

TABLE 2. RESULTS OF ELECTRON-MICROPROBE ANALYSES OF Co-SUBSTITUTED PARGASITE

| | | | | |
|---|---|---|---|---|
| $SiO_2$ wt.% | 34.86 | 36.07 | 37.47 | 35.92 |
| $Al_2O_3$ | 16.16 | 17.93 | 18.85 | 16.38 |
| CoO | 29.56 | 29.65 | 27.01 | 29.04 |
| CaO | 10.43 | 10.97 | 11.46 | 10.82 |
| $Na_2O$ | 3.55 | 3.60 | 3.60 | 3.34 |
| Total | 94.56 | 98.22 | 98.39 | 95.50 |
| Si *apfu* | 5.87 | 5.81 | 5.92 | 5.95 |
| Al | 3.21 | 3.40 | 3.51 | 3.20 |
| Co | 3.99 | 3.83 | 3.42 | 3.86 |
| Ca | 1.88 | 1.89 | 1.94 | 1.92 |
| Na | 1.16 | 1.12 | 1.10 | 1.07 |
| Total | 16.11 | 16.05 | 15.89 | 16.00 |

Formulae are based on 23 atoms of oxygen. *apfu*: atoms per formula unit.

The fine-grained nature of the synthetic Co-substituted pargasite made EMP analysis difficult, resulting in low totals (70–80%). Of the thirty analyses made, only four were of sufficient quality to give reliable compositions. Results are shown in Table 2. All have excess Al, up to 17% relative to the ideal formula, but otherwise approach the nominal end-member stoichiometry quite closely. Within analytical error, all four formulae have an amphibole stoichiometry. The proportion of [6]Al ranges from 1.08 to 1.43 *apfu* (atom per formula unit), and the *M*(4) site has up to 5% Na and 4% Co substitution for Ca.

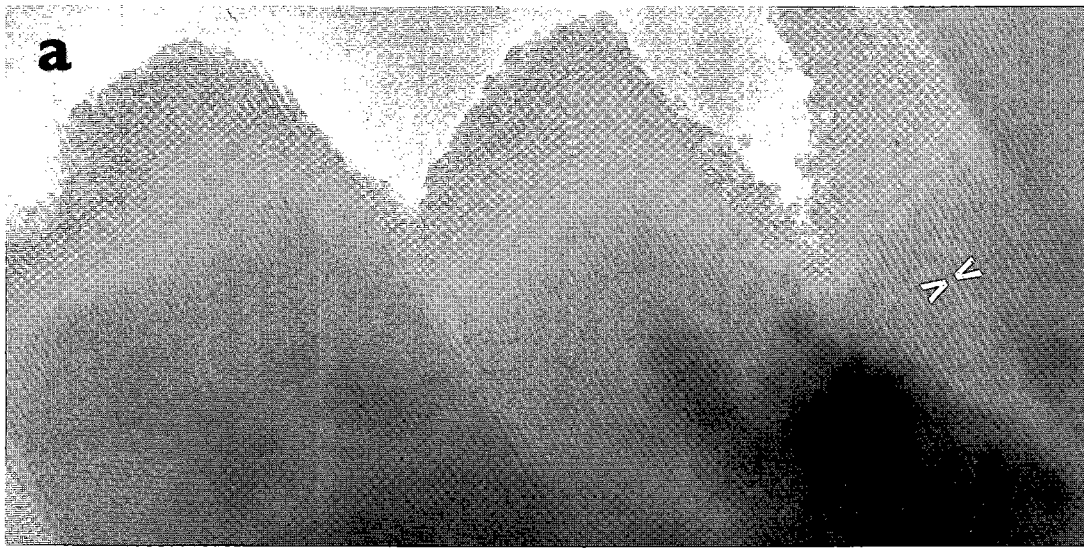

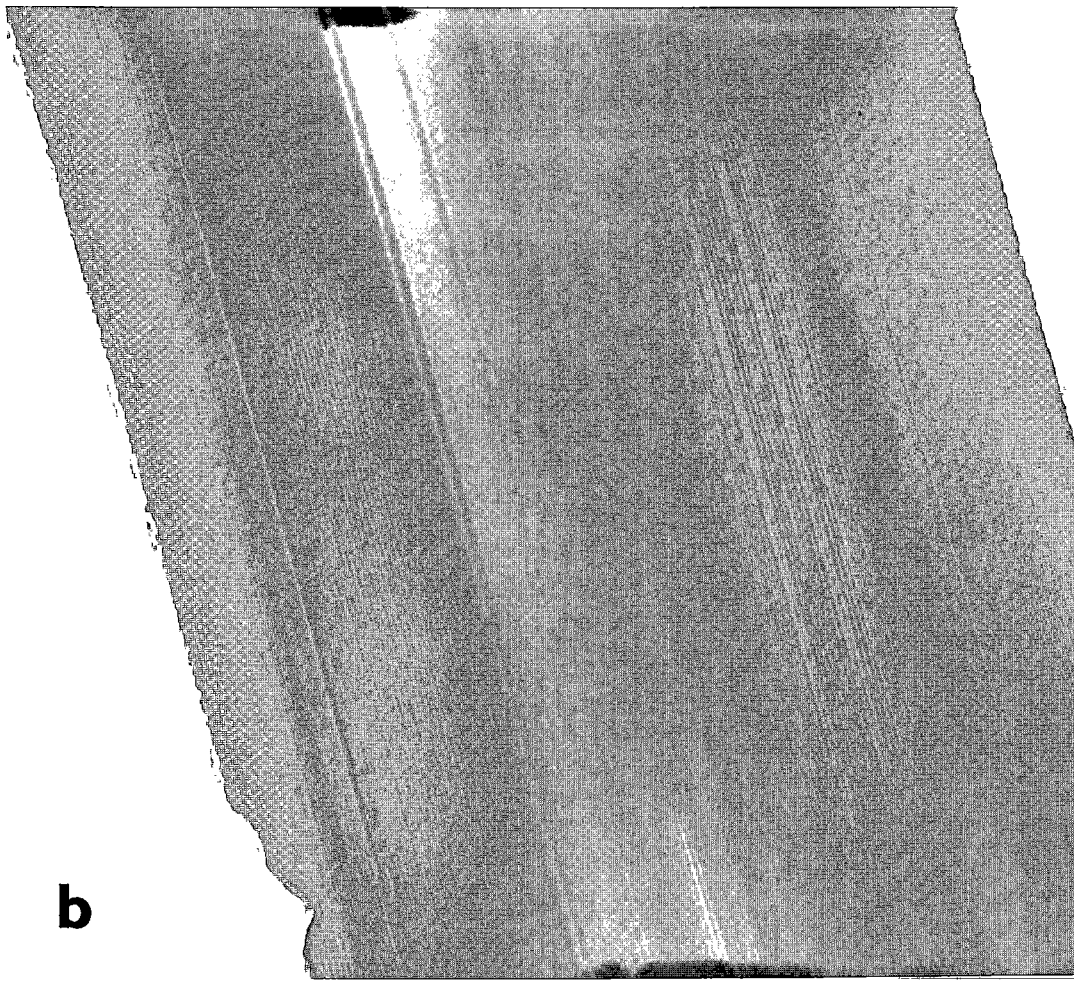


FIG. 1. HRTEM images of synthetic Co-substituted pargasite. (a) Edge of a larger amphibole grain showing a monotonous sequence of double chains characterized by the 9-Å lattice fringes (indicated by arrows). (b) Smaller crystallite of amphibole showing abundant CMFs with multiplicities of 3 and 4. About half of the crystal has the amphibole structure.

*Infrared spectroscopy*

The OH-spectra of the end-member pargasite are given in Figure 2; the OH groups in higher-multiplicity polysomes (see above) cannot significantly contribute to the pattern of Figure 2b because of their minor proportion over the bulk sample. Moreover, these OH groups would locally be in a mica-like environment and their vibrational frequency would overlap with the vibration of the OH groups of Co-substituted pargasite (Robert 1981), slightly affecting the intensity but not the multiplicity of the bands. The spectrum of synthetic pargasite is well known (Semet 1973, Raudsepp *et al.* 1987, Welch *et al.* 1994). It shows (Fig. 2a) a doublet consisting of two main bands of almost equal intensity, centered at 3710 and 3678 $cm^{-1}$. The band at 3710 $cm^{-1}$ is assigned to a configuration MgMgMg–OH–$^{[A]}$Na, *i.e.*, to a configuration with only Mg at *M*(1,3); the 3678 $cm^{-1}$ band is assigned to a configuration MgMgAl–OH–$^{[A]}$Na, *i.e.*, to a configuration involving Al at *M*(1,3). Additional shoulders on the low-wavenumber side of the 3678 $cm^{-1}$ band suggest the presence of a third component, centered at around 3650–3640 $cm^{-1}$ and strongly overlapping with the 3678 $cm^{-1}$ band. This component indicates the presence of vacant *A*-sites in the amphibole (Raudsepp *et al.* 1987, Della Ventura *et al.* 1998).

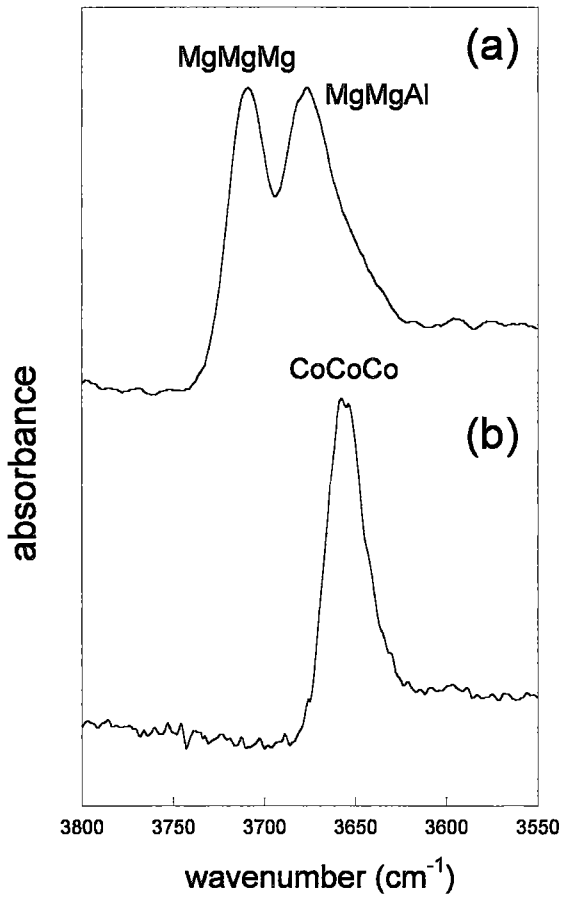


FIG. 2. FTIR spectra of (a) pargasite; (b) Co-substituted pargasite.

The spectrum of Co-substituted pargasite (Fig. 2b) shows a single rather asymmetrical band centered at 3656 $cm^{-1}$. It is shifted by 54 $cm^{-1}$ toward lower frequencies with respect to the MgMgMg–OH–$^{[A]}$Na band of pargasite. In synthetic sodic and potassic Co-substituted richterites, the CoCoCo–OH band is shifted 54 $cm^{-1}$ toward lower frequencies with respect to the MgMgMg–OH band (Della Ventura *et al.* 1996, 1997). For this reason, the band at 3656 $cm^{-1}$ in the spectrum of Co-substituted pargasite can be assigned to the CoCoCo–OH–$^{[A]}$Na configuration. It is worth noting that the same shift has also been observed in (Mg, Co)-substituted phlogopite (Robert 1981). For such substitutions, the frequency shift thus is the same for micas and amphiboles, in accord with the fact that the two structure-types are locally very similar in the neighborhood of the OH site.

The most interesting feature of the spectrum of Co-substituted pargasite is the absence of a second band toward lower wavenumber. This finding indicates that in Co-substituted pargasite, there is no Al at the $M(1,3)$ sites. Thus infrared spectroscopy shows Al to be completely ordered at $M(2)$ in this case.

*Unit-cell parameters*

Unit-cell dimensions of the two amphiboles are given in Table 3. Unit-cell data for synthetic pargasite along the Mg–Fe join are given in Charles (1980); those for the end-members are also listed in Table 3 for comparison. Figures 3 and 4 show the cell parameters of synthetic pargasite as a function of the mean cation radius at $M(1,2,3)$ (the cube of the mean-cation radius for the cell volume in Fig. 4), calculated assuming nominal

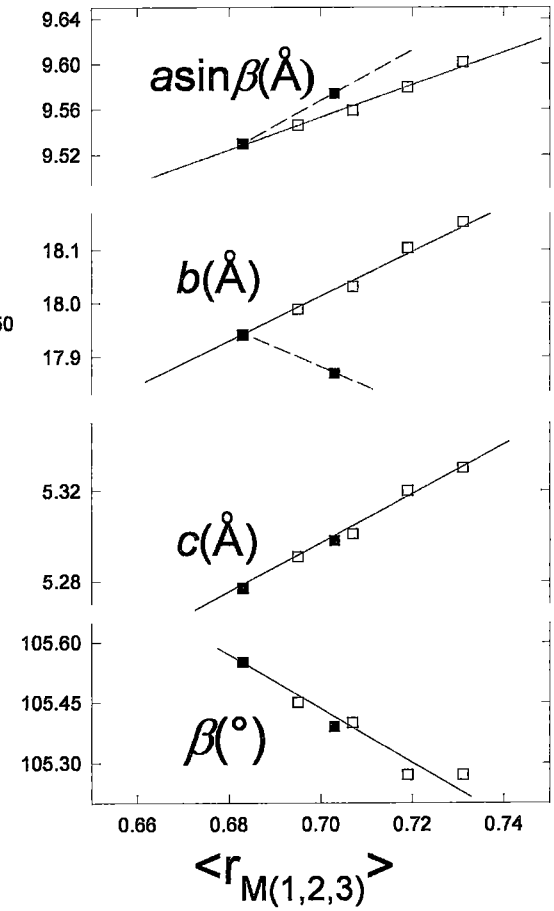


FIG. 3. Cell dimensions of synthetic pargasite along the Mg–Co–$Fe^{2+}$ join as a function of the mean cation-radius at $M(1,2,3)$. Filled squares: this work; open squares: data from Charles (1980).

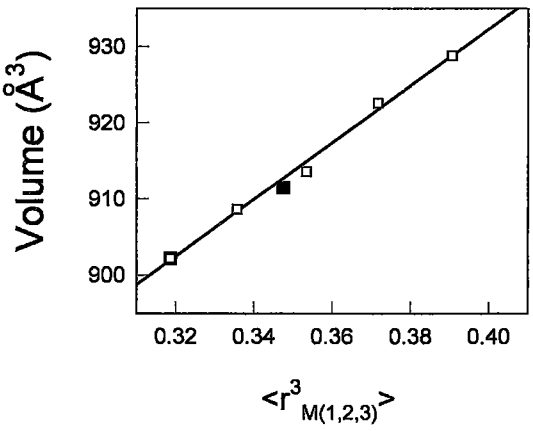


FIG. 4. Cell volumes of synthetic pargasite along the Mg–Co–$Fe^{2+}$ join as a function of the cubed mean cation-radius at $M(1, 2, 3)$. Symbols as in Figure 3.

compositions. It is well known that the mean sizes of the ions in the various structural positions significantly affect cell dimensions in clinoamphiboles (Colville *et al.* 1966). Accordingly, substitution of larger cations ($Co^{2+}$ = 0.745 Å; $Fe^{2+}$ = 0.780 Å) for the smaller Mg [r = 0.720 Å; all ionic radii values from Shannon (1976)] should cause an increase in the cell dimensions. This is the case, but the cell-parameter changes are very anisotropic. Along the Mg–Fe join, there is a linear trend for all cell parameters. For Co-substituted pargasite, there is a marked departure from this trend: $a\sin\beta$ is larger than expected, and $b$ is significantly shorter. The variation in cell volume is linear, and the β angle decreases linearly.

Similar behavior has been observed in (Mg, Co)-substituted potassium-richterite (Della Ventura *et al.* 1993a). For richterite-group amphiboles, there are data along the complete Ni–Mg–Co–Fe joins (Charles 1974, Della Ventura *et al.* 1997), which indicate that the trend is linear across the Ni–Mg–Fe system, and significant departure from linearity is observed only where Co is introduced into the structure. Following Della Ventura *et al.* (1993a), we conclude that the electronic configuration must be considered as a major factor affecting cell-parameter variation in transition-metal amphiboles. The behavior of the cell volume indicates that the relative anisotropy of expansion across the Mg–Co–Fe join is such that the expected monotonic increase in volume with increasing size of cation is maintained.

For richterite-group amphiboles, the greatest nonlinear behavior is observed for the $a$ and $b$ parameters, whereas here we observe a marked *decrease* of the $b$ dimension (Fig. 3). For clinoamphiboles, the $b$ unit-cell dimension is very sensitive to the site population at the $M(2)$ site (Colville *et al.* 1966). However, the substitution of the larger Co for the smaller Mg results in a *decrease* of the $b$ parameter in Co-substituted pargasite. Both the infrared spectrum and the results of the Rietveld structure refinement indicate that $^{[6]}Al$ is ordered at the $M(2)$ site in Co-substituted pargasite. Thus, the ideal $M(2)$ site population is $Co_{1.0}Al_{1.0}$ with a mean ionic radius of 0.640 Å, whereas in synthetic pargasite, the corresponding values are $Mg_{1.5}Al_{0.5}$, $\langle r\rangle$ = 0.674 Å [assuming that $M(3)$ is occupied by 0.50 Mg + 0.50 Al]. Thus Co-substituted pargasite has a smaller aggregate cation at the $M(2)$ site than pargasite, and hence the $b$ unit-cell dimension is smaller in Co-substituted pargasite than in pargasite, despite the fact that $Co^{2+}$ is larger than Mg. This is an excellent example of the anisotropic effect of cation order on the variation in cell dimensions in a structure.

TABLE 3. CELL PARAMETERS AND VOLUMES FOR SYNTHETIC PARGASITE AND RELATED SPECIES

| | 1 | 2 | 3 | 4 |
|---|---|---|---|---|
| $a$ (Å) | 9.897(3) | 9.930(1) | 9.892(1) | 9.953(5) |
| $b$ (Å) | 17.940(5) | 17.869(2) | 17.941(2) | 18.152(3) |
| $c$ (Å) | 5.279(2) | 5.2980(7) | 5.277(1) | 5.320(2) |
| β (°) | 105.54(4) | 105.39(1) | 105.55(1) | 105.27(2) |
| $V$ (Å³) | 903.0(4) | 911.46(1) | 902.2(3) | 928.8(4) |

1) synthetic Mg-end-member pargasite, this work.
2) synthetic Co-substituted pargasite, this work.
3) synthetic Mg-end-member pargasite, Charles (1980).
4) synthetic Fe-end-member ferropargasite, Charles (1980).

*Site occupancies*

Refined occupancies of the octahedrally coordinated sites for Co-substituted pargasite are given in Table 4. Studies of synthetic pargasite (Raudsepp *et al.* 1987) and richterite (Della Ventura *et al.* 1993a, b) indicate that the Rietveld method provides accurate site-populations for synthetic amphiboles. In the Co-substituted pargasite studied here, $M(3)$ is fully occupied by Co (Table 4), and only a small amount of Al occurs at $M(1)$; the $M(2)$ site is occupied by Co and Al in equal amounts. Several attempts were made to introduce anorthite or a more sodic plagioclase as a third phase in the refinement, but occupancies of the octahedra did not change significantly. In particular, the $M(2)$ and $M(3)$ site populations always converged (within standard error) to the values given in Table 4; the $M(1)$ occupancy was the most affected, but it was still found to converge around 0.90. Thus Rietveld refinement of Co-substituted pargasite shows that Al is essentially ordered at $M(2)$, in accord with the IR data (Fig. 2).

## DISCUSSION

The infrared spectrum of synthetic pargasite indicates that $^{[6]}Al$ is disordered over more than one of the $M(1,2,3)$ sites, whereas both the infrared spectrum and

TABLE 4. REFINED OCTAHEDRON OCCUPANCIES IN Co-SUBSTITUTED PARGASITE

| | *M*(1) | *M*(2) | *M*(3) | Occupancy |
|---|---|---|---|---|
| Co | 0.89 | 0.51 | 0.96 | 3.76 |
| Al | 0.11 | 0.49 | 0.04 | 1.24 |

Rietveld structure refinement of synthetic Co-substituted pargasite indicate that [6]Al is ordered at the *M*(2) site. Oberti *et al.* (1995) have shown that crystals of natural pargasite poor in Fe show [6]Al disorder over the *M*(2) and *M*(3) sites, and that the degree of this disorder is inversely related to the amount of $Fe^{2+}$ in the crystal. Hawthorne (1995) has argued that much of the disorder observed in nominally end-member amphiboles is driven by the need to maintain a significant entropy contribution to the free energy of the crystal. As a consequence of this, pargasite, an amphibole for which yields are high in syntheses, and which is close to end-member composition (Raudsepp *et al.* 1991), has a disordered distribution of [6]Al. Oberti *et al.* (1995) showed that there are severe bond-valence constraints on the occupancy of *M*(1) by Al in the local absence of $O^{2-}$ at the O(3) site, and hence [6]Al disorders over the *M*(2) and *M*(3) sites in pargasite. However, this tendency to disorder decreases as the Mg content of pargasite decreases. There are two aspects to this point: (1) with increasing $Fe^{2+}$-for-Mg substitution, there is an increasing entropy contribution to the free energy due to disorder; (2) as $Fe^{2+}$ increases, the yield of amphibole in synthesis experiments decreases, suggesting that the composition increasingly deviates from ideal stoichiometry. Point (1) is not relevant to Co-substituted pargasite, except that increasing $Fe^{2+}/(Fe^{2+} + Mg)$ has a grossly similar geometrical effect on the structure for a composition such that $r(Mg,Fe^{2+}) = r$Co (Fig. 4). However, the yield for the Co-substituted pargasite (~ 90%) is less than that obtained for pargasite, suggesting that the composition deviates more from that of the ideal end-member than pargasite. As there is no band attribuable to Co-substituted tremolite in the IR spectrum (Fig. 2b), the composition must deviate in the following manner: $NaCa_2(Mg_{4-x}Al_{1+x})(Si_{6-x}Al_{2+x})O_{22}(OH)_2$, $x > 0$; in this regard, the Rietveld site-populations sum to give $x = 0.24$ (Table 4).

There is an important additional point here pertaining to the geometrical effect of the increasing size of the octahedrally coordinated divalent cations with increasing $Fe^{2+}$-for-Mg substitution that parallels the replacement of Mg by $Co^{2+}$ in the structure of Co-substituted pargasite. The ionic radius of $Co^{2+}$ is 0.745 Å, corresponding to an $(Mg:Fe^{2+})$ ratio of 5:4. Examination of the curves of Oberti *et al.* (1995) shows that, for this composition (*i.e.*, geometrically equivalent to that of the Co-substituted pargasite end-member), there is no significant Al disorder over *M*(2) and *M*(3); [6]Al is completely ordered at *M*(2). Thus the relative degrees of [6]Al disorder exhibited by synthetic pargasite and Co-substituted pargasite are completely compatible with the range of disorder observed in analogous natural amphiboles. This indicates that the degree of this disorder is strongly related to the mean radius of the octahedrally coordinated divalent cations in pargasite.

## Conclusions

(1) Infrared spectroscopy shows [6]Al to be disordered over the *M*(1), *M*(2) and *M*(3) sites in synthetic pargasite.

(2) Infrared spectroscopy shows [6]Al to be ordered at the *M*(2) site in synthetic Co-substituted pargasite.

(3) Rietveld structure-refinement show virtually complete ordering of [6]Al at *M*(2) in synthetic Co-substituted pargasite, in agreement with IR spectroscopy.

(4) Correlation of these results with those obtained on natural samples of pargasite (Oberti *et al.* 1995) indicates that [6]Al disorder over *M*(2) and *M*(3) in the structure is inversely related to the mean ionic radius of the [6]-coordinated divalent cations.

(5) The *b* cell dimension of synthetic Co-substituted pargasite is less than that of synthetic pargasite despite the fact that $Co^{2+}$ is a larger cation than Mg. The aggregate size of the *M*(2) cation in Co-substituted pargasite [(1.0 Co + 1.0 Al)/2 = 0.640 Å] thus is smaller than the corresponding aggregate cation in pargasite [(1.5 Mg + 0.5 Al)/2 = 0.674 Å], and the size of the *b* cell-dimension is very sensitive to the size of the *M*(2) cation.

## Acknowledgements

Part of this work was done during the stay of GDV at the Department of Geological Sciences, University of Bristol, supported by a Royal Society Fellowship, within the exchange program of the Accademia Nazionale dei Lincei. GDV was supported by "Cofinanziamento MURTS 1997 – Relazioni tra struttura e proprietà dei minerali: analisi ed applicazioni". FCH was supported by Operating, Equipment and Infrastructure Grants from the Natural Sciences and Engineering Research Council of Canada and by a Killam Fellowship from the Canada Council. Thanks are due to P. Burns, H. Skogby and R.F. Martin for critical reading and helpful comments and to Michael Carroll for allowing the use of the FTIR spectrophotometer at the University of Bristol.

## References

Boyd, F.R. (1959): Hydrothermal investigations of amphiboles. *In* Researches in Geochemistry **1** (P.H. Abelson, ed.). John Wiley and Sons, New York, N.Y. (377-396).

BRAUE, W. & SECK, H.A. (1977): Stability of pargasite – richterite solid-solutions at 1 kb water vapour pressure. *Neues Jahrb. Mineral., Abh.* **130**, 19-32.

CAGLIOTI, G., PAOLETTI, A. & RICCI, F.P. (1958): Choice of collimators for a crystal spectrometer for neutron diffraction. *Nuclear Instr.* **3**, 223-228.

CHARLES, R.W. (1974): The physical properties of the Mg–Fe richterites. *Am.Mineral.* **59**, 518-528.

_____ (1980): Amphiboles on the join pargasite – ferropargasite. *Am. Mineral.* **65**, 996-1001.

COLVILLE, P.A., ERNST, W.G. & GILBERT, M.C. (1966): Relationships between cell parameters and chemical compositions of monoclinic amphiboles. *Am. Mineral.* **51**, 1727-1754.

DELLA VENTURA, G., HAWTHORNE, F.C., ROBERT, J.-L., DELBOVE, F., WELCH, M.D. & RAUDSEPP, M. (1998): Short-range order of cations in synthetic amphiboles along the richterite – pargasite join. *Eur. J. Mineral.*, in press.

_____, ROBERT, J.-L., BÉNY, J.-M., RAUDSEPP, M. & HAWTHORNE, F.C. (1993b): The OH–F substitution in Ti-rich potassium richterite: Rietveld structure refinement and FTIR and micro-Raman spectroscopic studies of synthetic amphiboles in the system $K_2O$–$Na_2O$–CaO–MgO–$SiO_2$–$TiO_2$–$H_2O$–HF. *Am. Mineral.* **78**, 980-987.

_____, _____ & HAWTHORNE, F.C. (1996) Infrared spectroscopy of synthetic (Ni,Mg,Co)- potassium-richterite. *In* Mineral Spectroscopy: a Tribute to Roger G. Burns (M.D. Dyar, C. McCammon & M.W. Schaefer, eds.). *The Geochemical Society, Spec. Publ.* **5**, 55-63.

_____, _____, RAUDSEPP, M. & HAWTHORNE, F.C. (1993a): Site occupancies in monoclinic amphiboles: Rietveld structure refinement of synthetic nickel magnesium cobalt potassium richterite. *Am. Mineral.* **78**, 633-640.

_____, _____, _____, _____ & WELCH, M.D. (1997): Site occupancies in synthetic monoclinic amphiboles: Rietveld structure-refinement and infrared spectroscopy of (nickel, magnesium, cobalt)-richterite. *Am. Mineral.* **82**, 291-301.

GILBERT, M.C. (1969): Reconnaissance study of the stability of amphiboles at high pressure. *Carnegie Inst. of Washington, Year Book* **67**, 167-170.

HAMILTON, D.L. & HENDERSON, C.M.B. (1968): The preparation of silicate compositions by a gelling method. *Mineral. Mag.* **36**, 832-838.

HAWTHORNE, F.C. (1995): Entropy-driven disorder in end-member amphiboles. *Can. Mineral.* **33**, 1189- 1204.

HILL, R.J. & HOWARD, C.J. (1986): A computer program for Rietveld analysis of fixed-wavelength X-ray and neutron diffraction pattern. *Australian Atomic Energy Commission (now ANSTO), Lucas Heights Research Laboratories (Menai, New South Wales, Australia), Rep.* **M112**.

HINRICHSEN, T. & SCHÜRMANN, K. (1977): Experimental investigations on the Na/K substitution in edenites and pargasites. *Neues Jahrb. Mineral., Abh.* **130**, 12-18.

HOLLOWAY, J.R. (1973): The system pargasite–$H_2O$–$CO_2$: a model for melting of a hydrous mineral with a mixed-volatile fluid. I. Experimental results to 8 kbar. *Geochim. Cosmochim. Acta* **37**, 651-666.

OBA, T. (1980): Phase relations on the tremolite – pargasite join. *Contrib. Mineral. Petrol.* **71**, 247-256.

OBERTI, R., HAWTHORNE, F.C., UNGARETTI, L. & CANNILLO, E. (1995): $^{[6]}$Al disorder in amphiboles from mantle peridotites. *Can. Mineral.* **33**, 867-878.

RAUDSEPP, M., TURNOCK, A.C. & HAWTHORNE, F.C. (1991): Amphibole synthesis at low pressure: what grows and what doesn't. *Eur. J. Mineral.* **3**, 983-1004.

_____, _____, _____, SHERRIFF, B.L. & HARTMAN, J.S. (1987): Characterization of synthetic pargasitic amphiboles ($NaCa_2Mg_4M^{3+}Si_6Al_2O_{22}(OH,F)_2$; $M^{3+}$ = Al, $Cr^{3+}$, Ga, $Fe^{3+}$, Sc, In) by infrared spectroscopy, Rietveld structure refinement and $^{27}$Al, $^{29}$Si and $^{19}$F MAS NMR spectroscopy. *Am. Mineral.* **72**, 580-593.

RIETVELD, H.M. (1969): A profile refinement method for nuclear and magnetic structures. *J. Appl. Crystallogr.* **2**, 65-71.

ROBERT, J.-L. (1981): *Etudes cristallochimiques sur les micas et les amphiboles. Applications pétrographiques et géochimiques.* Thèse d'Etat, Université Paris XI, Paris, France.

_____, DELLA VENTURA, G.C. & THAUVIN, J.-L. (1989): The infrared OH-stretching region of synthetic richterites in the system $Na_2O$–$K_2O$–CaO–MgO–$SiO_2$–$H_2O$–HF. *Eur. J. Mineral.* **1**, 203-211.

SEMET, M.P. (1973): A crystal-chemical study of synthetic magnesiohastingsite. *Am. Mineral.* **58**, 480- 494.

SHANNON, R.D. (1976): Revised effective ionic radii and systematic studies of interatomic distances in halides and chalcogenides. *Acta Crystallogr.* **A32**, 751-767.

WELCH, M.D., KOLODZIEJSKI, W. & KLINOWSKI, J. (1994): A multinuclear NMR study of synthetic pargasite. *Am. Mineral.* **79**, 261-268.

WESTRICH, H.R. & HOLLOWAY, J.R. (1981): Experimental dehydration of pargasite and calculation of its entropy and Gibbs energy. *Am. J. Sci.* **281**, 922-934.

WILES, D.B. & YOUNG, R.A. (1981): A new computer program for Rietveld analysis of X-ray powder diffraction patterns. *J. Appl. Crystallogr.* **14**, 149-151.

*Received May 7, 1998, revised manuscript accepted September 1, 1998.*